Pergamon

Adv. Space Res. Vol. 18, No. 7, pp. (7)37–(7)40, 1996
1995 COSPAR
Printed in Great Britain
0273–1177/96 $9.50 + 0.00

0273–1177(95)00287–1

ANGULAR EFFECT IN AVHRR'S SPLIT-WINDOW SEA SURFACE TEMPERATURE AND ATMOSPHERIC MOISTURE OVER THE ATLANTIC OCEAN

A. Ignatov and G. Gutman

Satellite Research Laboratory, NOAA/NESDIS, Washington, DC 20233, U.S.A.

ABSTRACT

The AVHRR on board NOAA satellites observes the underlying surface at different zenith angles within $\Theta \approx \pm 68°$ around nadir. The algorithms for retrieval of sea surface temperature (SST) t_s and the column water vapor content W from the angle-dependent brightness temperatures (BT) $t_i(\Theta)$ (i=4 and 5 for AVHRR Channels 4 and 5 with central wavelengths λ=10.8 and 12 μm, respectively) should overtly account for Θ to provide a result invariant of the variable observation geometry. Recently, a statistical method based on empirical angular functions (EAF) was proposed to assess the angular effect in both the original AVHRR BT's and retrieved SST and to test angular methods of SST retrieval /1/. The EAF's were employed to analyze the BT's in AVHRR Channels 3 and 4 and dual-window SST over tropical Atlantic in Jun 1987 and Dec 1988 from NOAA-10 and -11, respectively /1/. Here, we extend it to check the split-window SST and W, and the angular method of SST retrieval /2,3/, over the same target in tropical and an additional target in North Atlantic from NOAA-9 in Jul 1986.

CONCEPT OF EMPIRICAL ANGULAR FUNCTIONS (EAF)

BT in the i-th Channel $t_i(\mathbf{s};m)$ under cloud-free conditions depends upon the state of the ocean-atmosphere system (vector $\mathbf{s}$) and observation geometry ($m=\sec\Theta$ - relative air mass of the atmosphere). If the ocean and atmosphere were constant ($\mathbf{s}$=const) then BT would depend only on geometrical factor $t_i(\mathbf{s};m) \equiv t_i(m)$. We define that dependence as angular function. The simplified radiative transfer equation for aerosol-free atmosphere and non-reflective sea surface gives /4,5/:

$$t_i(\Theta) \approx t_s - (t_s - \bar{t}_a) \cdot W \cdot K_i \cdot m \qquad (1)$$

where $\bar{t}_a$ is the effective temperature of the atmosphere; K_i-absorption coefficient. According to (1), for a given vector $\mathbf{s}=\{t_s, \bar{t}_a, W\}$=const, $t_i(m)$ may be approximated linearly with respect to m. The derivation of the empirical angular function - EAF - from the top-of-the-atmosphere satellite measurements is, however, not trivial since it requires observations of a target with a constant SST through a constant atmosphere at many viewing angles Θ_k, k=1,..,K. The ATSR on board ERS1 allows viewing any target on the Earth surface at two angles $\Theta_1 \approx 0°$ and $\Theta_2 \approx 55°$ from two consecutive points of the orbit. The statistical procedure proposed in /1/ allows one to estimate the EAF's in the full range of AVHRR viewing angles. It is based on a histogram analysis of satellite data collected over a large quasi-uniform ocean region $S \sim (10°)^2$ which is stable enough during the time $\tau \sim 1$ month to allow multiple observations of S at different viewing angles. The BT's histograms are constructed using all satellite measurements over (S,τ) but separately for different angle bins $\Delta_k \equiv (m_k, m_k+\Delta m)$. The warm quasi-gaussian peak is associated with clear-sky views, and its mode $\bar{t}(\Delta_k)$ -- the mathematical expectation of the BT over (S,τ,Δ_k) domain -- corresponds to the mean ocean-atmospheric condition $\bar{\mathbf{s}}$. Estimation of the modes of histograms for different angle bins Δ_k (k=1,..,K) provides K points in the sought EAF, since all the mean values $\bar{t}(\Delta_k)$ are associated with the mean ocean-atmosphere state $\bar{\mathbf{s}}$, which is the same for different angle bins.

Application of the EAF. According to (1), the SST can be estimated either by a formal extrapolation of $t_i(m)$ to m=0 /2,3/ or as a linear combination of BT's in two channels. (1) underlies the NOAA's algorithm MCSST /6/ and suggested in /7/ algorithm for W retrieval

$$t_s = \alpha_1 \cdot t_4(m) + \alpha_2 \cdot t_5(m) + \alpha_0; \qquad W = A \cdot \{t_4(m) - t_5(m)\}/m \qquad (2,3)$$

where $A=[(K_{\lambda 5}-K_{\lambda 4})\cdot(t_s-\bar{t}_a)]^{-1}=1.96$ g·cm^{-2}·(°C)$^{-1}$ is assumed constant. The EAF's $t_4(m)$ and $t_5(m)$ enable one to check whether the linear approximation (1) holds and provides consistent intercepts in two channels, and the algorithms (2,3) result in angle-invariant SST and *W*.

DATA

In the present study, we use daily images from the NOAA's Global Vegetation Index (GVI) data set /8/. GVI is a subsample of Global Area Coverage (GAC) data mapped into a Plate Carree projection with a $(0.15°)^2$ lat/lon resolution. Since Apr 1985, it consists of global maps of the AVHRR counts in the Channels 1, 2, 4, and 5, as well as the associated scan and solar zenith angles. The GVI primary mission has been global vegetation studies (although the data over oceans was mapped also). As a result, the temperature was perceived to be of auxiliary role: the 10-bit GAC counts in Channels 4 and 5 are converted to the BT's T_4 and T_5 and further truncated to an 8-bit format /8/. This truncation results in a loss of accuracy: the GVI BT's are digitized with a step of 0.5°C for t≥-30°C. The non-linearity correction was done using the tabulated data of /9/. The absolute radiometric accuracy of resulting BT's is estimated to be no worse than 1°C. The described satellite BT data are far from ideal for EAF estimation because of low spatial resolution (an order of magnitude cruder as compared to GAC data and two orders cruder as compared to LAC) and crude 0.5°C-digitalization. We employed that data because of their convenient structure, and to provide a simpler consistent case for comparison with similar land studies which are underway. The statistical nature of the procedure implies that the use of high resolution data could improve the quantitative results of the present paper.

31 daily images from NOAA-9 for Jul 1986 were processed over two regions: S_1 in tropical Atlantic (10-20°N, 40-50°W -the same as used in /1/) and S_2 in N.Atlantic (50-62°N, 10-30°W). To estimate the homogeneity and stability over those regions, we used the SST-climatology /10/ which provides the multi-annual monthly means t_c and standard deviations σ_c within $(1°)^2$ grid boxes. That climatology contains 121 $(1°)^2$-boxes over S_1 and 271 over S_2, respectively. The mean $\bar{t}_c$ over S_1 and S_2 are 26.3 and 12.5°C, respectively. The value of σ_c, which characterizes the year-to-year variability in SST, is ≈1°C over tropical and ≈1.2°C over N.Atlantic. According to /10/, ~34% of the SST values can be expected between $\bar{t}_c$ and $\bar{t}_c+1\cdot\sigma_c$; ~14% between $\bar{t}_c+1\cdot\sigma_c$ and $\bar{t}_c+2\cdot\sigma_c$; and ~2% between $\bar{t}_c+2\cdot\sigma_c$ and $\bar{t}_c+3\cdot\sigma_c$, and a mirror image is found on the negative side of the mean. One should bear that in mind when comparing the results of SST retrieval with climatological values in the next Section. The spatial heterogeneity of the SST field within S_1 and S_2 is quantitatively described by standard deviations of t_c-values within S_1 and S_2 boxes of 0.5°C and 1.4°C, respectively.

The total AVHRR swath was subdivided into 18 angular bins (±9, symmetrically with respect to nadir) with an equidistant step of Δm=0.2. Crude filters (thresholding reflectances in Channel 1 and spatial uniformity tests in Channels 1 and 4) were used to exclude most obvious clouds, the objective being to clean up the peaks of the histograms to allow more reliable estimate of the position of the mode. An example of normalized smoothed histograms of the BT's over S_1 and S_2 for one angle bin is shown in Fig.1. Over tropical Atlantic, the shape is close to the Gaussian, similarly to described in /1/. Over the N.Atlantic, the two-peak shape indicates the presence of two clusters on the underlying surface. This feature is traced in almost every angle bin. We have fit this distribution with (bi)normal function

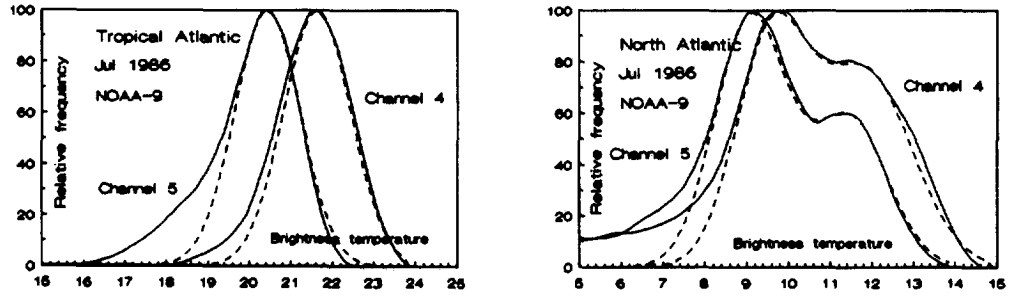

Fig.1. Histograms of BT's in Channels 4 and 5 in the near-nadir angular bin over tropical and N.Atlantic. Dashed lines show the results of their fitting by (bi)normal distributions.

TABLE 1. Statistics of the EAF's linear fit.

	Chan	Regression	R	σ, °C
Tropical Atlantic	4	24.0 - 2.0·m	0.99	0.19
	5	22.9 - 2.2·m	0.97	0.32
North Atlantic	4	11.5 - 1.8·m	0.93	0.39
	5	11.7 - 2.5·m	0.94	0.50

and have chosen the more statistically significant colder cluster assuming it represents typical conditions for this region, whereas the warm peak most probably results from Gulf Stream intrusion.

RESULTS

The results of the $\tilde{t}(\Delta_k)$ derivation are given in Fig.2. The histograms in two angular bins over tropical Atlantic were extremely wide and have been excluded from the analysis. The statistics of the linear fits are given in Table 1. The results over the second target are less accurate because of pronounced non-uniformity of underlying surface and persistent cloudiness. In tropics, intercepts in Channels 4 and 5 differ both from each other and the climatic SST (26.3°C) significantly. Over the N.Atlantic, extrapolation to m=0 provides SST more compatible with the climatic norm (12.5°C) in both Channels.

The operational in Jul 1986 split-window MCSST algorithm used the following formula: $t_s=3.4317 \cdot t_4 - 2.5062 \cdot t_5 + 1.58$ /11/. Substituting the t_4 and t_5 values from Table 1 for m=1 and 2 into this equation yields: t_s=25.2 and 23.8°C for tropics, and 11.8 and 11.9°C for the N.Atlantic, respectively. Thus, in high latitudes, MCSST for this particular case performs satisfactorily. In tropics, however, it underestimates the SST, with the descrepancy increasing with the viewing angle. The latter result agrees with the conclusion drawn in /1/ for the dual-window MCSST. The EAF's in split-window channels in tropical Atlantic are almost parallel, similarly to the dual-window ones, and no angle-independent coefficients in linear retrieval algorithm (2) can provide here angle-invariant SST. Use of the angle dependent coefficients was proposed in /12/. The model coefficients α_i were tabulated as a function of m for two samples of atmospheric situations representative for N.Atlantic and tropics. We applied those coefficients to the respective EAFs from Table 1, for m=1 and 2. The results are 24.9 and 24.5°C for tropics, and 10.8 and 11.4°C for N.Atlantic. The formulations /12/ treat angular dependence better than MCSST, yielding, however, the SST lower than both MCSST and the climatic norm.

Similarly to SST algorithms, one can check the algorithm for water vapor retrieval. Substituting EAF's from Table 1 into formula (3) for m=1 and 2 yields: W=2.5 and 1.5 g·cm^{-2} in tropics, and 1.0 and 1.2 g·cm^{-2} over N.Atlantic. W have no W-cimatology in cloudless conditions to validate the above values.

The angular effect in the retrieved SST and W is more pronounced in tropical regions. That may imply that the errors come most probably from simplified atmosphere treatment rather than the black surface approximation, used in deriving (1), because in tropical regions the warm downwelling radiance compensates for most of the deficit in emissivity, and additionally the surface signal is strongly attenuated by atmosphere, further depressing the effect of non-unit emissivity.

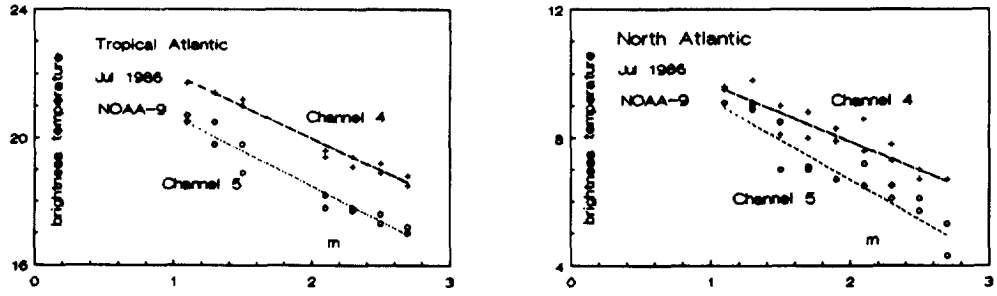

Fig.2. EAF's of BT's in Channels 4 and 5 and their linear fit over tropical and N.Atlantic.

CONCLUSION

The EAF's allow one to check consistency of different angular methods for SST retrieval in different spectral regions. The EAF's estimated over tropical Atlantic show that the results of extrapolation to zero air mass underestimate SST as compared to climatic norm in the region up to 2.5°C in Channel 4 and 3.5°C in Channel 5. For the N.Atlantic, the results of extrapolation in both channels are close to climatic SST within 1°C. The EAF's allow one to check whether the algorithms for the SST and W retrieval using cross-scanning radiometer data provide angle-invariant retrievals. Both the MCSST /6/ and water vapor /7/ retrieval algorithms fail to treat the angular effect in the extremal moist conditions. This result is in close agreement with the one obtained in /1/ over the same target in tropical Atlantic using two independent data sets. The accuracy of the EAF's derivation has to be improved. It can be done by using high-resolution satellite data of brightness temperatures with more precision. We plan to carry out similar analyses over selected land surfaces to assess the angular effect in the derived land surface temperature and water vapor over land. Theoretical and model analysis of the algorithms for the sea surface temperature and integral water vapor retrievals should go along with experimental studies.

Aknowledgements. Thanks go to Dr.G.Ohring (SRL) for critical review of the manuscript. D.Sullivan (Research and Development Corporation) helped us in organizing the AVHRR time series over the two oceanic targets, and P.Clemente-Colon (SRL) provided the SST-climatology. This work was done when A.I. held National Research Council Associateship at SRL, on leave from the Marine Hydrophysics Institute, Sevastopol, Crimea, Ukraine.

REFERENCES

1. A.Ignatov and I.Dergileva, Angular effect in dual-window AVHRR brightness temperatures over oceans. *Int.J.Rem.Sens.*, in press.

2. A.Gorodetsky, Estimation of surface temperature by the angular scanning method. *Issledovanie Zemli iz Kosmosa*, #2, 36-44 (1981, in Russian).

3. A.Chedin, N.Scott and A.Berroir, A single-channel double-viewing angle method for SST determination from coincident METEOSAT and TIROS-N radiometric measurements. *J.Appl.Meteor.*, 21(4), 613-618 (1982).

4. C.Prabhakara, G.Dalu and V.Kunde, Estimation of sea surface temperature from remote sensing in the 11- to 13-μm window region. *J.Geophys.Res.*, 79(33), 5039-5044 (1974).

5. L.McMillin, Estimation of sea surface temperatures from two infrared window measurements with different absorption. *J.Geophys.Res.*, 80(36), 5113-5117 (1975).

6. P.McClain, W.Pichel and C.Walton, Comparative performance of AVHRR-based multichannel sea surface temperature. *J.Geophys.Res.*, 90(C5), 11587-11601 (1985).

7. G.Dalu, Satellite remote sensing of atmospheric water vapor. *Int.J.Rem.Sens.*, 7(9), 1089-1097 (1986).

8. K.Kidwell, Global Vegetation Index User's Guide, U.S. Department of Commerce, National Oceanic and Atmospheric Administration, 49pp (1990).

9. M.Weinreb, G.Hamilton, S.Brown and R.Koszor, Nonlinearity corrections in calibration of Advanced Very High Resolution Radiometer infrared channels. *J.Geophys.Res.*, 95(C5), 7381-7388 (1990).

10. U.S.Navy Marine Climatic Atlas of the World, 1992. Naval Oceanography Command Detachment, Asheville, N.C., CD-ROM Ver. 1.0, March 1992.

11. I.Barton, Satellite-Derived Sea Surface Temperatures -- A comparison between operational, theoretical, and experimental results. *J.Appl.Meteorol.*, 31(5), 433-442 (1992).

12. D.Llewellyn-Jones, P.Minnett, R.Saunders and A.Zavody, Satellite multichannel infrared measurements of sea surface temperature of the N.E.Atlantic Ocean using AVHRR/2. *Quart.J.Roy.Meteor.Soc.*, 110, 613-631 (1984).